

Stabilization techniques for spinning rotor gage residual drag

Suk-Ho Choi,^{a)} Sharrill Dittmann, and Charles R. Tilford

National Institute of Standards and Technology, Center for Chemical Technology, Gaithersburg, Maryland 20899

(Received 21 July 1990; accepted 22 May 1990)

The pressure-independent residual drag on a spinning ball requires an offset correction for the accurate use of a spinning rotor vacuum gage (SRG) at low pressures. Instabilities in the residual drag (RD) can cause significant errors in low-pressure SRG measurements. The instabilities usually occur as discontinuous shifts when a ball is levitated by the magnetic suspension, or as continuous changes as the ball slows down. The discontinuous shifts in residual drag have been found to be caused by changes in the orientation of the ball's magnetic moment, induced by the suspension field or the inductive drive circuit. Premagnetizing the ball in a strong field has stabilized the orientation of the magnetic moment and the RD value. The continuous changes are caused by competition between magnetic and inertial forces, which result in a frequency-dependent orientation of the rotational axis of the ball. Etching a spot on the ball alters its shape and defines an inertial axis. Magnetizing the ball in a preferred direction with respect to this axis minimizes both the residual drag and its frequency dependence.

I. INTRODUCTION

Commercial molecular drag gages, commonly known as viscosity, spinning ball, or spinning rotor gages (SRGs), can be used throughout the high-vacuum range. The operation of these gages, which has been described in detail elsewhere,¹ is as follows: A bearing ball, typically 4.5 or 4.76 mm ($\frac{3}{16}$ in.) in diameter and fabricated from a magnetic material, is magnetically levitated, spun up to about 400 Hz by an inductive drive, and allowed to coast. The rotation rate of the ball can be determined using a signal induced by a rotating component of the ball's magnetic moment in a set of pickup coils. Collisions between gas molecules and the surface of the ball will cause the ball to slow down at a fractional rate determined by the ball's moment of inertia, the gas molecular mass, the temperature of the gas, the average tangential momentum transfer per collision, and the gas density or pressure. However, even at zero pressure the rotation rate will change, generally decreasing with time, although small rates of increase can also be observed for some balls. Very small rates of change (usually unobservable) can be caused by Coriolis, thermal noise, or relativistic effects.² However, readily observable changes are due to temperature-induced changes in the ball's moment of inertia, particularly following spin-up of the ball by the inductive drive,³⁻⁶ and small but observable changes, discussed later, are due to second-order interactions between the SRG suspension circuitry and the ball. However, the primary effect is the residual drag (RD) generated by induced eddy currents. These are of two types: eddy currents induced in the ball by asymmetries about the axis of rotation in the magnetic suspension field (which causes what we shall call the suspension-field residual drag, or SFRD), and eddy currents induced in surrounding metallic components by the rotating component of the ball's magnetic moment (which causes what we shall call the rotating-moment residual drag, or RMRD).

Ignoring the small Coriolis and relativistic effects, the second-order instrument interactions, and the temperature-induced changes in the moment of inertia, the SRG pressure

relationship can be derived from gas-kinetic theory and elementary mechanics:

$$P = \sqrt{8kT/\pi m} (r\rho\pi/10\sigma_{\text{eff}}) (-\dot{\omega}/\omega) - \text{RD}, \quad (1)$$

where k is Boltzmann's constant, T is the absolute temperature of the gas, m is the gas molecular mass, r is the radius of the ball, ρ is the density of the ball, σ_{eff} is the average fraction of tangential momentum transfer per collision (effective accommodation coefficient, typically close to 1), and $\dot{\omega}/\omega$ is the measured fractional rate of change of the ball's rotation rate or angular speed. Note that the residual drag can be measured and discussed in terms of the fractional rate of slowing of the ball's rotation rate, or in terms of the equivalent pressure. Throughout this text RD will be given in terms of the equivalent nitrogen pressure.

The residual drag is different for each ball and suspension head, and the RMRD may change significantly each time a ball is suspended, or spun-up by the inductive drive. Typically, the residual drag is equivalent to a nitrogen pressure between 10^{-4} and 10^{-3} Pa, although higher and lower values are commonly observed. The residual drag is taken into account by measuring the indicated SRG pressure at "zero" pressure (any pressure less than the desired pressure measurement resolution) and entering this number into the SRG control unit as an "offset correction," which is then automatically subtracted from subsequent measurements. Since typical values of the residual drag are orders of magnitude larger than the imprecision, about 10^{-6} Pa, of an SRG, instability of the residual drag can be the primary factor limiting the low-pressure performance of the SRG.

For some balls, as long as the ball is left suspended and rotating, the residual drag will be stable at the level of 10^{-6} Pa or less for periods of a day or more; however, for other balls, changes may be much larger than this. Significant changes can be observed for most balls each time the magnetic suspension is energized and the ball picked up; for some balls the residual drag will steadily decrease as the ball slows down, and occasionally the residual drag will change and/or

the frequency dependence change when the inductive drive is briefly energized in order to drive a slow ball back up to a preferred operating frequency.

We will demonstrate that the frequency dependence of the residual drag is due to frequency-dependent changes in the axis of rotation, caused by a competition between magnetic and inertial forces on the ball, with consequent changes in the RMRD. We will further demonstrate that the changes in residual drag when the ball is resuspended or the inductive drive turned on are due to changes in the direction and/or magnitude of the ball's magnetization. We describe techniques whereby the magnetization and principal moment of inertia can be established and stabilized in a preferred orientation, resulting in small and stable residual drags.

II. THEORY OF THE ROTATING-MOMENT RESIDUAL DRAG

The behavior of a rotating SRG ball can be modeled, as illustrated in Fig. 1, by assuming that it has a magnetic moment μ displaced by an angle θ from the axis of rotation and the angular velocity vector ω , which is aligned with the direction of the suspension magnetic field, \mathbf{B} . The magnitude of the RMS voltage, V , induced in a pickup coil will be proportional to the changing magnetic flux from the rotating ball, and will be

$$V = C_1 \mu \omega \sin \theta, \tag{2}$$

where μ and ω are the magnitudes of μ and ω , and C_1 is a constant which depends on the geometry and location of the pickup coil. The fractional rate of rotational slowing, $-\dot{\omega}/\omega$, due to the energy dissipated by the current induced in surrounding conductors, that is, the RMRD, will be given by

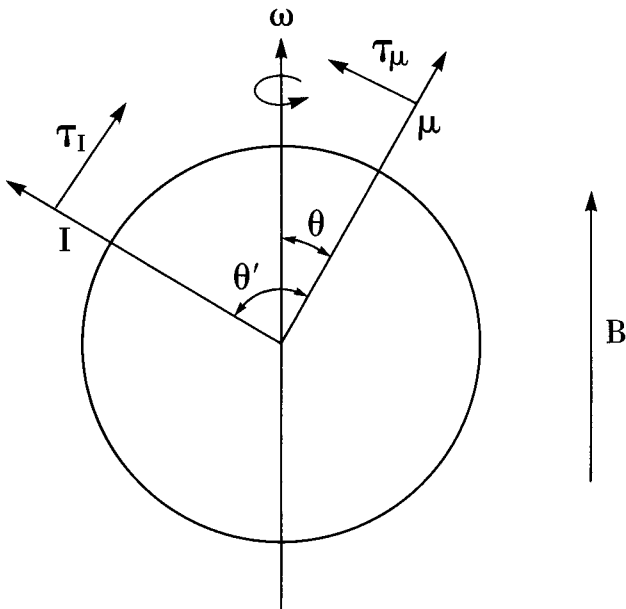


FIG. 1. Model of a spinning rotor gauge ball. ω is the axis of rotation, parallel to the suspension field, \mathbf{B} . μ is the magnetic moment, and \mathbf{I} is the direction of the largest principal moment of inertia.

$$\text{RMRD} = C_2 \mu^2 \sin^2 \theta, \tag{3}$$

where C_2 depends on the geometry and conductivity of the material surrounding the rotating ball.

While both C_1 and C_2 depend in a complicated manner on the geometry of the pickup coil and the surrounding conducting material, Eqs. (2) and (3) are completely general in predicting the dependence on μ , ω , and θ of the magnitude of the timing signal and the RMRD.

The alignment of the spin axis of the ball, or the magnitude of θ , is determined by two competing torques. The interaction of the magnetic field, \mathbf{B} , and the magnetic moment, μ , generates a torque $\tau_\mu = \mu \times \mathbf{B}$, with magnitude $\tau_\mu = \mu B \sin(\theta)$, which tends to align the magnetic moment with the spin axis of the ball. If the ball were perfectly spherical and homogeneous this alignment would occur (this would have the undesirable result that the rotating component of the magnetic moment, and the signal used to determine the rotation rate, would both be zero). However, no real ball is perfectly spherical. The asymmetries of the ball generate a frequency-dependent inertial torque that tends to align the axis of the largest principal moment of inertia with the spin axis. In Fig. 1 the largest principal moment is shown oriented in the direction \mathbf{I} , at an angle θ' with respect to the magnetic moment. The inertial torque is given by $\tau_I = \omega \times \hat{\mathbf{I}} \cdot \omega$, where $\hat{\mathbf{I}}$ is the inertia tensor.

The asphericity of the ball can be modeled by assuming that a small mass η is removed from the surface of a perfectly spherical ball of radius r , at the point where \mathbf{I} intersects the surface. The magnitude of the inertial torque will then be $\tau_I = \eta r^2 \omega^2 \sin(\theta' - \theta) \cos(\theta' - \theta)$.

Equating the two torques we find the relationship

$$\omega^2 = (2\mu B / \eta r^2) \sin(\theta) / [\sin(2\theta') \cos(2\theta) - \sin(2\theta) \cos(2\theta')]. \tag{4}$$

For an SRG ball, typical values are $\eta \approx 60 \mu\text{g}$, $\mu \approx 2 \times 10^{-4} \text{ J m}^2/\text{wb}$, $B \approx 0.06 \text{ T}$ (600 G), and $r \approx 2.38 \text{ mm}$. For these values the dependence of θ on ω and θ' is illustrated in Fig. 2. The values of θ are close for values of θ' symmetric about 45° , e.g., for $\theta' = 1$ and 89° , particularly at the low-

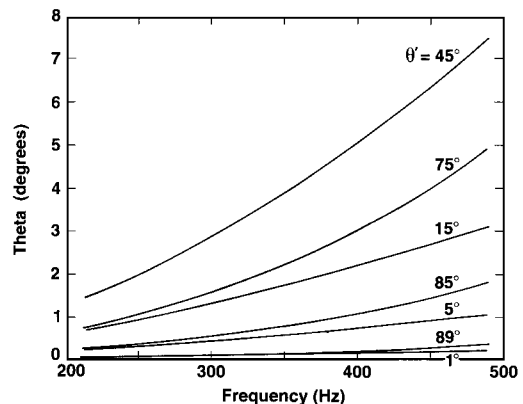


FIG. 2. Calculated dependence of θ , the angle between the magnetic moment and the rotation axis, on frequency and θ' , the angle between the magnetic moment and the largest principal moment of inertia. Parameters for a typical SRG were assumed.

er frequencies. Further for values of θ' close to 0° or 90° , θ is very small, as is its dependence on rotation rate. This indicates that the RMRD, and the signal voltage, should both decrease as θ' approaches 0° or 90° , although the RMRD will decrease at a faster rate.

At low frequencies the values of θ are small for all values of θ' and we can approximate Eq. 4 to obtain

$$\sin \theta \approx \frac{1}{2} \eta r^2 \omega^2 \sin(2\theta') / [\mu B + \eta r^2 \omega^2 \cos(2\theta')].$$

For values of θ' close to 0° we can further approximate to obtain

$$V \approx C_1 \frac{1}{2} \mu \omega^3 \eta r^2 (2\theta') / (\mu B + \omega^2 \eta r^2) \quad (5)$$

and

$$\text{RMRD} \approx C_2 \frac{1}{4} \mu^2 \eta^2 r^4 \omega^4 (2\theta')^2 / (\mu B + \omega^2 \eta r^2)^2. \quad (6)$$

For values of θ' close to $\pi/2$ (90°) we obtain

$$V \approx C_1 \frac{1}{2} \mu \omega^3 \eta r^2 (\pi - 2\theta') / (\mu B - \omega^2 \eta r^2) \quad (7)$$

and

$$\text{RMRD} \approx C_2 \frac{1}{4} \mu^2 \eta^2 r^4 \omega^4 (\pi - 2\theta')^2 / (\mu B - \omega^2 \eta r^2)^2. \quad (8)$$

These equations predict that as θ' approaches 0° the RMRD will approach zero at a faster rate than the signal voltage and that at lower frequencies the RMRD will vary with the fourth power of ω . For a typical SRG ball $\mu B = \omega^2 \eta r^2$ for $\omega \approx 5900$ rad/s (950 Hz). Therefore, at the SRG operating frequencies around 400 Hz the denominator of Eq. (6) will typically be within a factor of 2 of that of Eq. (8), so we expect that as θ' approaches 90° or $\pi/2$ the behavior will be similar to the behavior near 0° . However, at higher frequencies, or larger values of η , the RMRD for a ball magnetized near 90° will become much larger than for a ball magnetized near 0° . The behavior of the RMRD as a function of θ' and ω is illustrated in Fig. 3, using the exact Eqs. (3) and (4). The rapid decrease of the RMRD for values of θ' near 0° or 90° is evident.

At low frequencies, for all values of θ' , there is a significant fractional frequency dependence of the RMRD. However, for values of θ' close to 0° or 90° , the RMRD is so small that the absolute variation of the RMRD with frequency will be

very small, as illustrated in Fig. 4. Figure 4 was obtained by a numerical differentiation of Fig. 3.

This analysis indicates that the RMRD can be minimized and stabilized with respect to frequency if the angle between the magnetic moment and the inertial moment of the SRG ball is close to 0° , and that similar results will be obtained, for typical SRG operating parameters, if the angle is close to 90° . However, both of these conditions will also reduce the timing signal, and may cause the accuracy of the timing to decrease and the random errors of the measured pressure to increase.

III. EXPERIMENTAL PROCEDURES

In order to evaluate the accuracy of this theoretical model and develop techniques to stabilize the residual drag, it was necessary to determine the direction of the magnetic moment and the principal moment of inertia of the balls, and measure their residual drag. For this purpose we used the two types of ball materials commonly used with SRGs; "normal" or "chrome" steel (such as SAE 52100) and "stainless" steel (such as 440C). The balls were production $\frac{3}{16}$ -in.-diam bearing balls; the stainless steel balls were grade 5, and the normal steel balls were grade 10 or 16. This means that all diameters are within 5, 10, or 16 μ in., respectively, of the specified diameter.

The direction and character of the magnetic moment was determined by mounting the ball on an aluminum shaft or spindle driven by a stepping motor, and mounting a Hall-probe Gaussmeter close to the equator of the ball. The output of the Gaussmeter and the drive signal for the stepping motor were used to drive an X-Y plotter, giving a record of the magnetic field close to the surface of the ball as a function of angle at the equator.

The direction of the principal moment of inertia of the "as-received" balls could not be readily determined; even assuming a uniformly dense material, measurement of the ball diameters with sufficient accuracy would be very difficult. Therefore, the principal moment was determined by deliberately changing the shape of the ball. Previous efforts

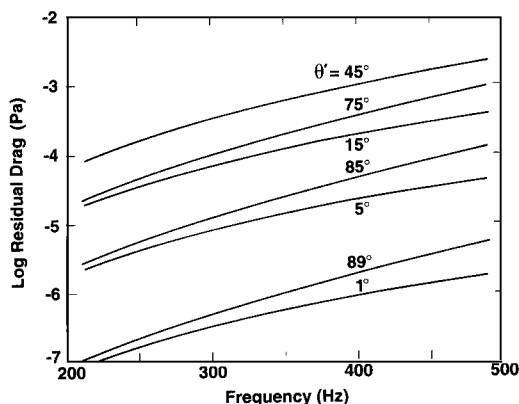


FIG. 3. Calculated rotating-moment residual drag (RMRD) as a function of frequency and magnetization angle. Magnitude of the residual drag has been determined by normalizing to a typical experimental value at 400 Hz for a ball magnetized at 45° .

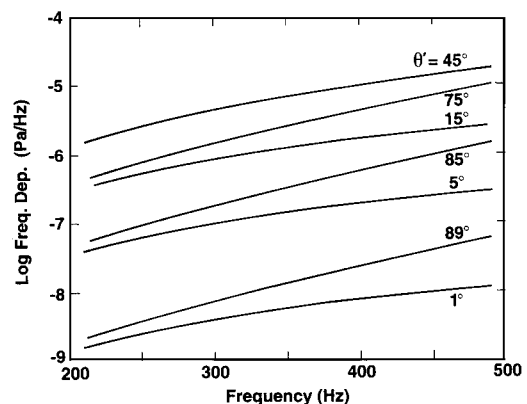


FIG. 4. Calculated frequency dependence of the rotating-moment residual drag (RMRD) as a function of frequency and magnetization angle. These data were obtained by a numerical differentiation of the curves in Fig. 3.

to do this by “sanding” or grinding a small flat spot on the ball invariably removed too much material and the resultant balls could not be made to spin in a stable manner. We found that we could control the material removal much better using a chemical etch (aqua regia; $\text{H}_2\text{O}:\text{HCl}:\text{HNO}_3 = 15:5:4$). The location of the material removal was controlled in two different ways. In the first of these, the ball was coated with wax, and a small circle scratched in the wax with a fine needle before the ball was immersed in the etching solution.

The second, and much more successful technique, used a set of two Teflon blocks, into each of which a $\frac{3}{16}$ -in. hemispherical cavity was milled. A 1-mm-diam hole was drilled through each Teflon piece to the pole of the hemispherical cavity. A set of aluminum jigs was used to tightly clamp a ball in the cavity formed by the two Teflon pieces so that the Teflon sealed to the ball. A hypodermic needle was then used to place etching solution on the ball surface exposed at the bottom of one or both of the 1-mm-diam holes, which are at opposite ends of a diameter through the ball. Etching times of from 1 to 4 h were used for the normal steel balls, resulting in the removal of 40–140 μg of material. Similar etching times were used for the stainless steel balls—this would remove 15–65 μg of material. We estimate that the maximum asphericity in a grade 16 ball would be equivalent to the removal of about 75 μg from one position on the ball, therefore the material removed by the etching should be the primary determinant of the direction of the inertial moment. The etched spot(s) is visible to the naked eye and serves as a reference point for future measurements on the ball.

As discussed below, initial measurements showed that the direction of the magnetic moment could be stabilized only by premagnetizing the ball in a strong field. For this purpose the aluminum clamping jig was prepared with surfaces milled at different angles with respect to the axis determined by the etched spot(s), so that the orientation of the ball could be controlled in the magnetizing field.

Two different turbomolecular-pumped vacuum systems were used to establish the “zero” pressure required for residual drag determinations. They had nitrogen equivalent base pressures of less than 5×10^{-7} Pa. Residual drag measurements were made using commercial SRG controllers. After the balls were spun-up, a minimum of 5 h was allowed for the temperature perturbation caused by the inductive drive to attenuate. Measurements were then made of the indicated nitrogen pressure, with no offset correction. A residual drag of 10^{-5} Pa corresponds to a decrease in the rotation rate of 0.2 Hz/day at 400 Hz; therefore, for balls with a small RD it was necessary to artificially slow the balls between data points in order to obtain the RD frequency dependence. This was done by increasing the pressure in the system so that the molecular drag slowed the ball the desired amount, and then reducing the pressure back to “zero” before the next data point.

Measurements were made both with commercial SRG suspension heads, and a special head⁵ with dimensions about twice those of the standard commercial head. This special or “low-drag” head was designed for improved suspension field symmetry in order to reduce the component of the residual

drag, SFRD, due to field asymmetries, and to space the conducting components of the suspension head further away from the rotating magnetic field of the ball.

Typically, 30-s sampling times were used, and ten readings were taken and averaged every 30 min under microcomputer control. During the measurements the room temperature typically varied no more than $\pm 0.5^\circ\text{C}$ with a time constant of 15–30 min, causing an insignificant temperature effect in the data.

IV. RESULTS AND DISCUSSION

A. Magnetization

The magnetic field at the surface of several balls was mapped with reference to the etched spot or some other reference mark on the surface using the previously described Gaussmeter and spindle apparatus. Two such mappings were required to determine the magnitude and location of the maximum field, and the orientation of the dominant magnetic moment. After determining the location of the peak field in the first mapping, the ball is reoriented so that the axis of rotation and the peak field location during the first mapping are now on the equator of the ball. This should ensure that the maximum field is now located on the equator of the ball during the second rotation. Typical results are illustrated for a normal or chrome steel ball in Fig. 5; the field strengths given in the figure legend are the maximum fields measured at the surface of the ball. In the “as-received” condition the field is of the order of a few tenths of a gauss (a few tens of microteslas), as seen in curve 1. After suspension of the ball using the SRG suspension head and control unit, the maximum field is of the order of 12–13 G for a normal steel ball, as seen in curve 2, and 7–8 G for a stainless steel ball. If the balls are resuspended the magnitude of the field changes very little, but the orientation of the

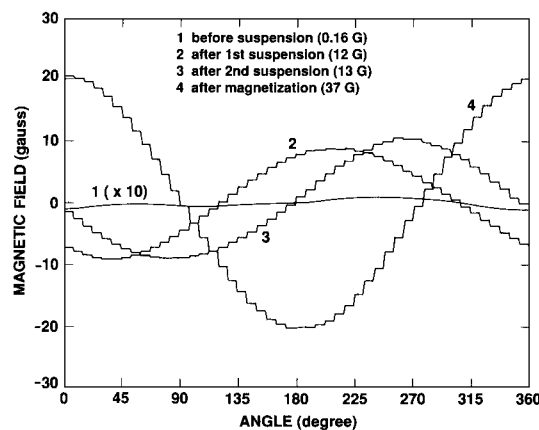


FIG. 5. Magnetic field about the equator of a chrome or normal steel (SAE 52100) SRG ball. The difference between curves 2 and 3 are typical of the random shifts that occur each time an as-received ball is suspended. Curve 4 is after magnetization in a 3.5-kG field and is not altered by suspension of the ball. Maximum field strengths at the surface are indicated in the legend for each curve. The discontinuities in the data are due to the discrete steps of the motor used to rotate the ball with respect to the Hall probe.

maximum field changes in a completely random manner, as illustrated by the shift of curve 3 from curve 2. These random changes will recur with repeated suspensions. The change of magnetization direction with each suspension explains the observation⁶ that the RD value and its frequency dependence can change whenever the ball is resuspended.

In an attempt to stabilize the magnetic moments of the balls they were premagnetized using a 3.5-kG permanent magnet. Curve 4 of Fig. 5 illustrates the magnetic field after this premagnetization. Both the magnitude and orientation of this field remained unchanged after repeated suspensions and over periods of months. However, the field magnitude, but not the orientation, decreased with exposure to high temperatures. After baking under vacuum at 100 °C for 167 h the field decreased by 20%. Baking at 150 °C for 70 h caused a decrease of 55% and baking at 200 °C for 15 h caused a decrease of 75%. Thus, premagnetization will stabilize the magnetic moment of the balls, but baking temperatures and times must be limited in order to maintain this condition. The direction of the magnetization could be changed by placing the ball back in the 3.5-kG field at a different angle; data were obtained on a number of balls that were successively magnetized at different angles.

The magnetic field curves for the normal or chrome steel balls were very sinusoidal, indicating that the magnetic moment can be approximated by a simple dipole. However, significant deviations from a sinusoid were observed for stainless-steel balls; the angular difference between the maximum and minimum fields differed from 180° by as much as 22°–31°. This indicates that their magnetic structure is more complex than the simple dipole model.

B. Residual drag and frequency dependence

In order to test the predictions of Sec. II a series of normal and stainless-steel balls were etched, with one or two spots on a diameter, and premagnetized at angles of 0°, 45°, and 90° with respect to the diameter through the etched spot(s). Data obtained from balls prepared using the “wax and scratch” technique showed larger variations than that from

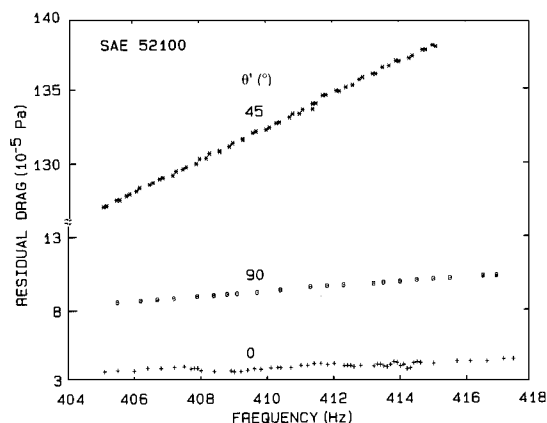


FIG. 6. Residual drag as a function of frequency for a normal steel ball successively magnetized at angles of 0°, 45°, and 90° with respect to an etched spot.

balls etched and magnetized using the Teflon and aluminum jig. This is probably due to the less precise control of the etching and magnetization obtained with the first technique, therefore, data obtained from these balls are not included in the data presented below. However, data from the “wax and scratch” balls are entirely consistent with the conclusions drawn from the data presented below.

It should be noted that if the simple-dipole model is correct and the angle between the magnetic moment and inertial moment, θ' , is 0° or 90°, the magnetic moment will line up with the spin axis (at low frequencies), there will be no timing signal, and the ball will be useless in an SRG. However, θ' differs from the angle between the etched spot and the premagnetization for several reasons, principally because the initial asphericity of the ball will cause the moment of inertia to deviate from the etched spot, and the magnetic field of the permanent magnet deviates from the normal to the pole piece. Therefore, balls etched and magnetized at angles of 0°, 45°, and 90° can only be said to have θ' close to these values.

Figure 6 illustrates the residual drag as a function of frequency of a normal steel ball that was etched and successively premagnetized at angles of 0°, 90°, and 45°. It is apparent that both the residual drag and the frequency dependence are much larger for 45° than they are for 0° and 90°. For all three angles the results could be replicated after repeated resuspensions. Note that the data include an SFRD contribution that presumably is constant, independent of the magnetization angle.

Figure 7 shows the residual drag for five different normal steel balls variously magnetized at 0°, 45°, and 90°. The residual drag of each ball was determined using one of several different standard SRG suspension heads and the low-drag head. As in Fig. 6, the residual drags at 0° and 90° are significantly less than those at 45°. This difference is most marked when comparing the results for a particular ball that has been successively magnetized at all three angles. Similar, but less marked differences were observed for stainless-steel balls. For a given ball, magnetized at 0° or 90°, the residual drag using the low-drag head is significantly less than that

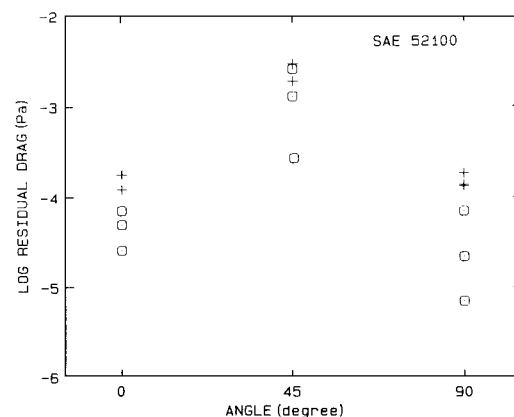


FIG. 7. Residual drag as a function of magnetization angle (θ') for five normal steel balls. Measurements were made both with standard suspension heads (+), and a low-drag head (O), and multiple measurements were made for some balls after magnetization at different angles.

determined using a standard head, demonstrating that the SFRD component of the residual drag is significantly lower for the low-drag head.

Figure 8 illustrates the residual drag for a number of normal and stainless-steel balls magnetized at 0° and 90° . It is apparent that the normal steel balls consistently have lower residual drags than the stainless-steel balls (this difference is less evident for balls magnetized at 45°). We believe this is because the magnetic structure of the stainless-steel balls is more complicated. The simple-dipole model is not applicable, and even when premagnetized in a certain direction, significant magnetization may occur in other directions. For this reason, most of our data were taken with normal steel balls, and we have not included much of the stainless-steel ball data in this paper. The results for the stainless-steel balls are consistent with those from the normal steel balls, but the correlation between magnetization angle and residual drag is not as clear as it is for the normal steel balls.

Not shown in any of the figures are several apparent negative values of residual drag that were observed during these experiments (negative residual drags are not physically possible). These negative offset corrections are occasionally observed with standard SRG suspension heads and balls that have not been premagnetized; we observed negative values a number of times using the low-drag head and balls magnetized at 0° or 90° . Fremerey and Lindenau⁷ have suggested that this energy gain is due to a second-order interaction between the sensing current in the SRG vertical detection circuitry and the rotating ball. This interaction pumps a small amount of energy into the ball that, depending on the direction of the ball's rotation, will slowly increase or retard the rotation rate of the ball. In the first case, if the true residual drag is small, the ball will actually speed up with time, resulting in an apparent negative residual drag. At Fremerey and Lindenau's suggestion, we have verified this hypothesis by varying the sensing current in the vertical detection circuitry and observing corresponding changes in the indicated

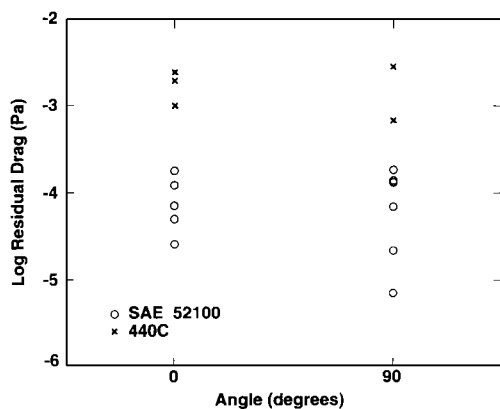


FIG. 8. Residual drag as a function of magnetization angle (θ') for the five normal steel balls (O) of Fig. 7 and five stainless-steel balls (X). Some normal steel balls were measured both with a standard suspension head and with the low-drag head, as detailed in Fig. 7. The stainless-steel balls were all measured with the low-drag head. The systematically larger values for the stainless-steel balls are believed due to a more complicated magnetic structure.

residual drag. In most cases, the negative indicated pressures could be eliminated by reducing the sensing current to half its normal value. In order to obtain the true residual drag the sensing current would have to be reduced to zero. For practical use this perturbation of the apparent residual drag is not a problem since it is small and should remain constant with time.

The data of Fig. 6 appear to be linear with frequency, while Eqs. (6) and (8) indicate that at low frequencies the RD values should vary as the fourth power of frequency. We believe this apparent linearity is largely due to the limited frequency range of Fig. 6; we have analyzed data between 300 and 400 Hz for a ball magnetized at 45° and find that at low frequencies it is well represented by an ω^4 dependence, with significant deviations from this functional form starting around 350 Hz, and increasing with frequency. However, for practical purposes, within small frequency intervals, the frequency dependence can be represented by a linear function, with the linear coefficient obtained from a least-squares fit to the data.

Figure 9 shows the linear frequency dependence of the residual drag between 405 and 415 Hz for the same balls presented in Fig. 7. As can be seen, the frequency dependence is about two orders of magnitude less for balls magnetized at 0° and 90° , compared to balls magnetized at 45° . Data for normal steel balls prepared using the "wax and scratch" technique are very much the same, data for stainless-steel balls are similar, but the correlation is not as strong. The magnitude of the frequency dependence for $\theta' = 0^\circ$ or 90° does not systematically depend on whether standard or low-drag suspension heads are used.

As noted before, balls magnetized at a specified angle with respect to an etched spot will have θ' values that are only close to the magnetization angle. Comparison of the experimental results presented in Figs. 6, 7, and 9 with the theoretical predictions of Figs. 3 and 4 would indicate that balls magnetized at 0° or 90° have θ' values that are closer to 5° and 85° .

Theoretically, the behavior of a ball should be the same whether it is etched at one or both ends of a diameter, assuming that the same total amount of material is removed. Our results for a few balls that were etched at both ends of a

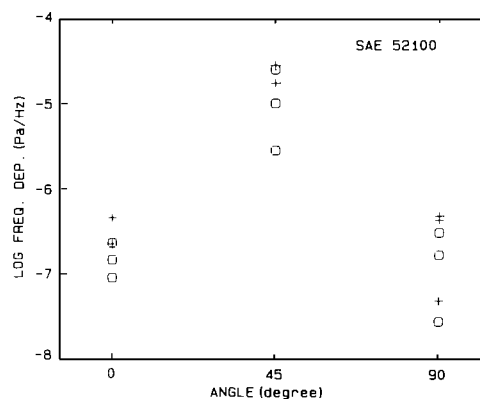


FIG. 9. Linear frequency dependence of the residual drags shown in Fig. 7.

diameter appeared to be the same as those for the majority of the balls that were etched at only one spot. It should also be noted that the effect of the etched spot on the effective accommodation coefficient is rather small for a ball magnetized parallel to the etched diameter. Since the etched spot will then be aligned with the axis of rotation, a 1-mm-diam spot will account for about 1% of the tangential momentum transfer.

C. Random errors

The previous results convincingly demonstrate that defining θ' close to 0° or 90° will minimize both the residual drag and its frequency dependence. However, as can be seen from Eqs. (5) and (7), as θ' approaches these values the magnitude of the induced signal used to time the rotation of the ball will also decrease, although at a slower rate. If the signal becomes too small, signal noise will cause increased random errors in the measurement of the rotation rate of the ball, and hence, of the pressure. These random errors can be evaluated from the standard deviation of repeated measurements of the residual drag. These are shown in Fig. 10 for the normal steel balls, and as can be seen, the random errors do not significantly increase as the residual drag decreases; in fact, the largest standard deviations were obtained for balls with residual drags greater than 5×10^{-3} Pa, prepared using the wax and scratch technique and not included in Fig. 10. Apart from this, the available data for all balls indicate no significant correlation between random errors and either angle of magnetization or residual drag. It is also not possible to distinguish between the results obtained with the low-drag suspension head and the standard heads.

V. CONCLUSIONS

The residual drag of a SRG ball will depend on the orientation of the ball's magnetic moment with respect to the axis of rotation. The changes in residual drag that typically occur each time a ball is suspended, and that occasionally occur when the drive circuit is energized, are due to changes in the ball's magnetization caused by the suspension field, or the field from the inductive drive. These changes can be prevented by premagnetizing the ball in a strong field. The simple-dipole model also predicts that the residual drag and its frequency dependence can be minimized if the magnetic moment is either very nearly parallel or perpendicular to the axis of the largest principal moment of inertia of the ball. Experimental results for normal steel balls agree well with this model, although the imprecision of the data did not allow us to verify the prediction that the residual drag and its frequency dependence would be smaller for parallel than for perpendicular magnetizations. The behavior of stainless-steel balls was less predictable. We believe this is because the magnetic structure of the stainless-steel balls is more compli-

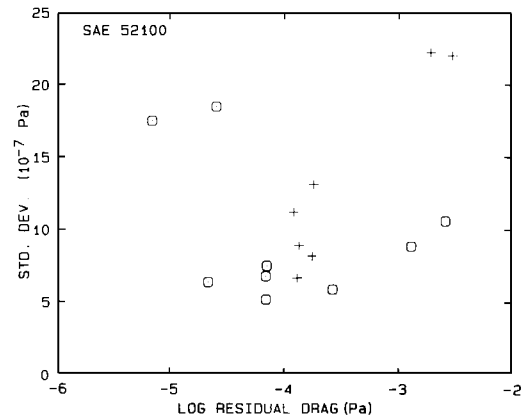


FIG. 10. Standard deviations about the mean for the residual drags shown in Fig. 7. Sampling times were 30 s and 10 readings were included in each data set.

cated than a simple dipole. The magnitude of the random error of the measured residual drag or pressure appears to be independent of the angle of magnetization.

These results indicate that in order to minimize instabilities in the residual drag the following steps should be taken: Normal or chrome steel balls should be used; the balls should be etched or otherwise modified to define the moments of inertia; and the balls should be magnetized in a strong field that is parallel, or nearly parallel, to the diameter through the etched spot. Nearly spherical (grade 5) balls should be used so that the etching more clearly defines the inertial moment, and baking temperatures should not exceed 100°C and baking times should be minimized in order to maintain the magnet moment.

ACKNOWLEDGMENTS

S.-H.C. appreciates support from the Korea Science and Engineering Foundation. This work was supported by the U.S. Department of Energy, Office of Fusion Energy, and benefited greatly from the assistance of A. R. Filippelli, F. G. Long, D. Martin, and R. Davis.

^aNIST Guest Researcher. Permanent address: Korea Standards Research Institute, P.O. Box 3, Daedok Science Town, Daejeon 305-606, Republic of Korea.

¹J. K. Fremerey, *J. Vac. Sci. Technol. A* **3**, 1715 (1985).

²See, for example, J. K. Fremerey, *Phys. Rev. Lett.* **30**, 753 (1973); B. E. Bernard, L. I. Winkler, and R. C. Ritter, *Metrologia* **21**, 115 (1985).

³B. E. Lindenau, *Vacuum* **38**, 893 (1988).

⁴M. Hirata, H. Isogai, and M. Ono, *J. Vac. Sci. Technol. A* **4**, 1724 (1986).

⁵S. Dittmann, B. E. Lindenau, and C. R. Tilford, *J. Vac. Sci. Technol. A* **7**, 3356 (1989). The low-drag head was designed and built by the second author.

⁶K. E. McCulloh, S. D. Wood, and C. R. Tilford, *J. Vac. Sci. Technol. A* **3**, 1738 (1985).

⁷J. K. Fremerey and B. E. Lindenau (private communication).